Differential effects of prediction and adaptation along the cortical hierarchy during deviance processing

Running title: Hierarchical prediction errors in the human brain

Schlossmacher, Insa[1,2], Dilly, Jacky[1], Protmann, Ina[1], Hofmann, David[1], Dellert, Torge[1,2], Roth-Paysen, Marie-Luise[1], Moeck, Robert[1], Bruchmann, Maximilian[1,2], and Straube, Thomas[1,2]

[1]Institute of Medical Psychology and Systems Neuroscience, University of Münster, 48149 Münster, Germany

[2]Otto Creutzfeldt Center for Cognitive and Behavioral Neuroscience, University of Münster, 48149 Münster, Germany

Corresponding author:
Insa Schlossmacher
Institute of Medical Psychology and Systems Neuroscience
University of Münster
Von-Esmarch-Strasse 52
48149 Münster
Germany
Phone: +49 251 83-52785
Fax: +49 251 83-56874
E-mail: insa.schlossmacher@uni-muenster.de

Abstract

Neural mismatch responses have been proposed to rely on different mechanisms, including prediction-related activity and adaptation to frequent stimuli. However, the cortical hierarchical structure of these mechanisms is unknown. To investigate this question, we used functional magnetic resonance imaging (fMRI) and an auditory oddball design with a suited control condition that enabled us to delineate the contributions of prediction- or adaptation-related brain activation during deviance processing. We found that while predictive processes increased with the hierarchical position of the brain area, adaptation declined. This suggests that the relative contribution of different mechanisms in deviance processing varies across the cortical hierarchy.

Introduction

Detecting changes in our environment is a cornerstone of perception. A vast amount of research effort has been put into the investigation of neural correlates of deviance processing including neuroimaging (Kim, 2014) and electrophysiological approaches (Näätänen et al., 2011; Polich, 2007; Stefanics et al., 2014), showing increased activity to deviant stimuli in different variants of oddball designs. Recently, hierarchical predictive processing has been put forward as a theoretical underpinning for these deviance-related effects (Clark, 2013; Garrido et al., 2009; Stefanics et al., 2014; I. Winkler & Czigler, 2012). From this point of view, the increase of neural activation for unexpected rare stimuli compared to expected frequent ones stems from a comparison process where a prediction is compared with the actual sensory input. If prediction and input do not match, as is the case when a rare – and thus unexpected – deviant stimulus is presented, a prediction error signal would be elicited. This prediction error signal would then be propagated upwards in the hierarchy and compared with the predictions of the next higher level and so forth, enabling efficient information processing (Clark, 2013; Stefanics et al., 2014).

However, while predictive processing offers a compelling explanation for deviance-related effects, it is not the only process that could be responsible for an observed difference between rare and frequent stimuli. Stimulus-specific adaptation has also been proposed to play an important role during deviance processing (Jääskeläinen et al., 2004; May & Tiitinen, 2010; Nelken, 2014). In this theoretical framework, the difference between rare and frequent stimuli stems from habituation of neuronal responsiveness to the frequent stimulus, which thus elicits a smaller response compared to the non-adapted cells (fresh afferents) activated by the rare stimulus. In other words, deviance responses in typical oddball designs are not driven by genuine mismatch responses but by altered, i.e., reduced responses to the standard stimulus.

At first glance, prediction and adaptation seem opposing. However, there is evidence

that both processes can be present in the brain to variable degrees in the same region or at the same time (Ishishita et al., 2019; Laufer et al., 2008; Opitz et al., 2005; Parras et al., 2017). One way to delineate the contribution of these two mechanisms to deviance effects is to compare the responses of deviant and standard stimuli to a control stimulus (Maess et al., 2007; Parras et al., 2017; Schröger & Wolff, 1996). The control stimulus is usually physically identical to the deviant but presented in a multi-standard paradigm where all stimuli are displayed with the same stimulus probability as the deviant. Comparing the deviant with the control thus offers a way to distill deviance-related activity without being contaminated by adaptation. Additionally, comparing the control with the standard stimulus shows adaptation-related activity.

Using this experimental procedure, there is initial evidence from an electrophysiological study in rodents (Parras et al., 2017) that the relative contribution of prediction vs. adaptation increases from subcortical areas to auditory cortex. In line with these results, two neuroimaging studies specifically targeting the auditory cortex showed the presence of both mechanisms within Heschl's gyrus and superior temporal gyrus (STG) with an anterior-posterior gradient in humans (Laufer et al., 2008; Opitz et al., 2005). Furthermore, an electrocorticography (ECoG) study found that temporal areas were related to predictable changes, while frontal areas indexed unpredictable changes (Dürschmid et al., 2016). However, to date, there are no brain imaging studies that investigated the effects of prediction vs. adaptation across all typical cortical brain areas commonly showcasing deviance-related effects (Kiehl et al., 2005; Kim, 2014). Besides primary and secondary auditory cortex, encompassing Heschl's gyrus and STG, several frontal and parietal areas included in ventral and dorsal attention networks, as well as subcortical areas, reliably show increased activation to deviant vs. standard stimuli (Kiehl et al., 2005; Kim, 2014). Thus, deviance responses are processed on different hierarchical levels traversed during auditory processing from the thalamus to Heschl's gyrus and STG and onwards to higher order association cortices (Li et al., 2019; Parras et al., 2017).

This hierarchical dimension of deviance processing, i.e., whether and how mechanisms

vary depending on the cortical region, has not been investigated yet. In order to address this gap, we conducted a high-powered fMRI study (n = 54) using an oddball design with a suited control condition that allowed to delineate prediction- and adaptation-related mechanisms in typical areas involved in auditory deviance processing in humans.

Methods

Participants

Fifty-nine right-handed participants with normal hearing and no history of neurological or psychiatric illness took part in the experiment and were compensated with €10/h. Four participants had to be excluded due to excessive head movements (> 3 mm) during recording and one participant because of anatomical MRI anomalies. The remaining 54 participants (39 female) were aged from 18 to 33 (M = 23.20, SD = 3.04). The local ethics committee has approved the study and all procedures were carried out in accordance with the Helsinki declaration.

Experimental procedure and stimulus material

Stimuli consisted of pure sine-tones of 600, 800, 1000, 1200, and 1400 Hz. Stimulus duration amounted to 100 ms, including rise/fall times of 10 ms. The sound volume was chosen to be easily audible during functional sequences but not unpleasantly loud. In oddball blocks, the 800 and 1200 Hz tones served as deviant and standard counterbalanced across participants. The probability of deviant to standard stimuli was 20:80 and stimulus presentation was pseudorandomized so that no two deviants were presented consecutively. In control blocks, all five tone stimuli were presented randomly with a probability of 20% (see Figure 1A). Throughout, participants' task was to respond to target stimuli of 300 ms duration, which were randomly interspersed in the sequence. In total, 40 targets were included, the frequency of which conformed to the stimulus probability of the current block, i.e., all tone frequencies could be potential targets. Interstimulus intervals ranged from 1.04 to 17.25 s (M = 3.01, SD = 2.06)

and were derived using optseq2 (Greve, 2009). Four different optseq sequences were computed and randomly assigned to two runs per participant, creating 12 different sequence combinations. In total, two runs of 250 stimuli (ca. 13 min each) were acquired and separated by a short break. One run could start with either an oddball or control block, which seamlessly changed to control or oddball block in the middle of the run. Whether the participants started with the oddball or control block was counterbalanced across participants. The second run was always presented in reverse order, e.g., if the first run was oddball-control, the second run was control-oddball. Before starting the experiment, a short practice block of about 1 min was presented in order to accustom the participants to the task. Stimuli in this practice block were structured like the experimental block that followed, i.e., they also included brief oddball and control sequences. At all times, a white fixation cross was presented on a black screen, and participants were asked to fixate during the run. Stimulus presentation and response collection were controlled by the

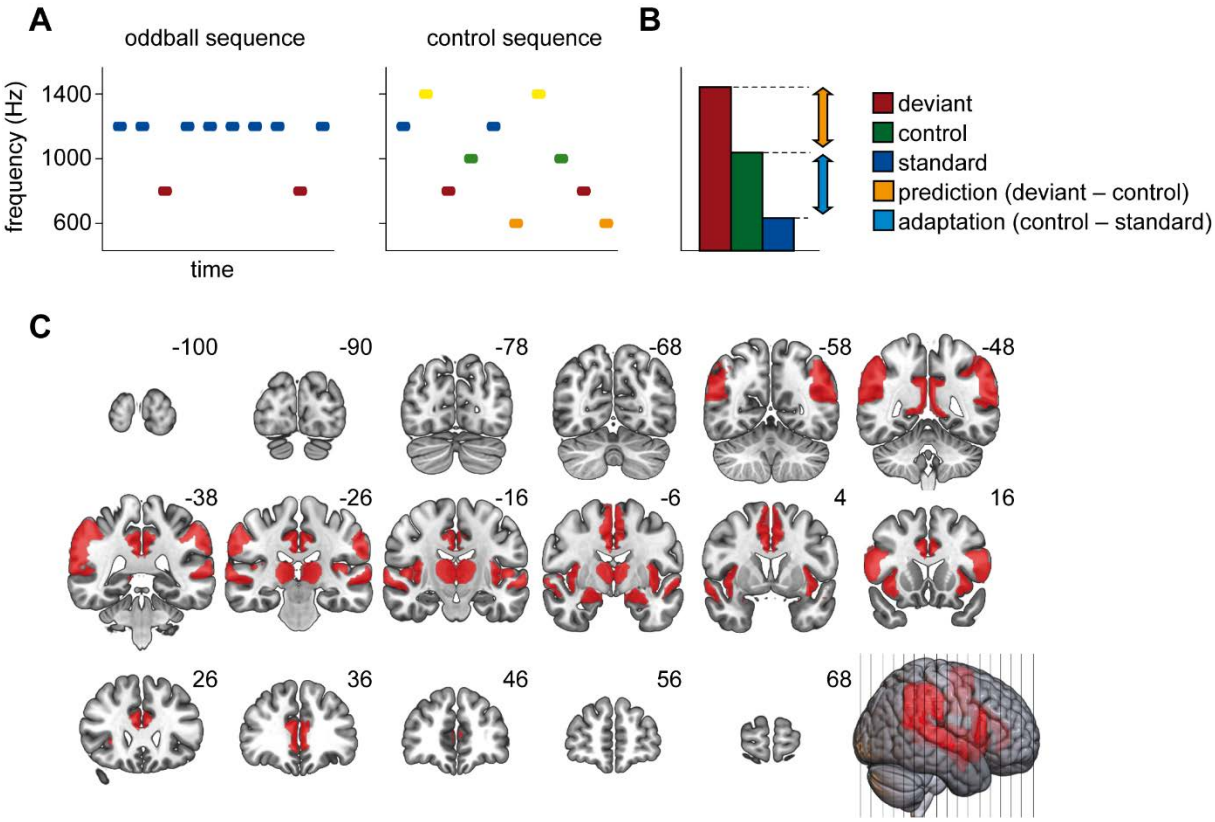

Figure 1. Experimental paradigm and mask for data analysis. (A) Schematic of oddball and control sequence. In the experiment, the frequencies of deviant and standard stimulus were counterbalanced across participants. (B) Decomposition of observed responses into prediction-related and adaptation-related activity. (C) Illustration of the mask applied during the cluster-based permutation. Red areas were included in the mask.

133 software Presentation (Version 21.1, Neurobehavioral Systems, Albany, CA).

134 **Data acquisition and preprocessing**

135 A 3-Tesla Siemens Magnetom Prisma with a 20-channel Siemens Head Matrix Coil
136 (Siemens Medical Systems, Erlangen, Germany) was used to aquire MRI data. In a first step,
137 we obtained a high-resolution T1-weighted scan with 192 slices for anatomical localization and
138 coregistration (repetition time (TR) = 2130 ms, echo time (TE) = 2.28 ms, flip angle (FA) = 8°,
139 field of view (FOV) = 256 × 256 mm, voxel size = 1 × 1 × 1 mm). A shimming field was applied
140 in order to minimize magnetic field inhomogeneity. Then, we recorded two functional datasets
141 per participant (2 runs) consisting of 353 volumes and 42 slices each by means of a T2*-
142 weighted echoplanar sequence sensitive to blood oxygenation level-dependent (BOLD)
143 contrast (TR = 2300 ms, TE = 30 ms, FA = 90°, FOV = 216 × 216 mm, voxel size = 3 × 3 × 3
144 mm).

145 Preprocessing relied on SPM12 v7771 (Wellcome Department of Cognitive Neurology,
146 London, UK) and the Data Processing & Analysis of Brain Imaging (DPABI) 4.3 toolbox (Yan
147 et al., 2016) in MATLAB. We removed the first five data volumes to account for spin saturation
148 effects. Then, slice-scan-time correction and realignment using a six-parameter (rigid body)
149 linear transformation was performed. In a next step, we co-registered anatomical and functional
150 images and segmented these into gray matter, white matter and cerebrospinal fluid. Finally, we
151 normalized functional data to Montreal Neurological Institute (MNI) standard space using
152 DARTEL (Ashburner, 2007), resampled it to 3 mm isotropic voxels and spatially smoothed it
153 with an 8 mm full width at half maximum Gaussian kernel.

154 **Statistical Analysis**

155 A general linear model (GLM) was estimated for each participant in the first-level
156 analysis. In order to eliminate slow signal drifts, we used a high-pass filter with a cutoff of 128
157 seconds. We applied SPM's pre-whitening method FAST (Corbin et al., 2018) to model
158 autocorrelations as recommended by Olszowy and colleagues (2019). The GLM design matrix

contained the onsets of deviants, standards, controls, targets and responses as predictors as well as six head movement parameters which represented predictors of no interest. We included two predictors accounting for the stimuli presented during the control condition. One used the onsets of the stimulus physically identical to the deviant (later compared with the deviant and standard), the other modeled the onsets of all other control stimuli. These onsets were then convolved with a 2-gamma hemodynamic response function to model the BOLD signal change for each predictor. Contrast images (deviant − standard) of the beta estimates were created for each participant for the second-level analysis.

In order to isolate mismatch-related activity in the second-level analysis, we used the cluster-based permutation as implemented in PALM (A. M. Winkler et al., 2014). The voxel-wise α amounted to .001; a cluster was deemed significant with $\alpha < .05$. The number of permutations was set to 10000. Based on the recent meta-analysis of Kim (2014), the following areas of interest were identified and included in one mask based on the Harvard Oxford Atlas (Desikan et al., 2006): Heschl's gyrus, superior temporal gyrus (STG), anterior and posterior cingulate cortex (ACC/PCC), supplementary motor area (SMA), inferior frontal junction (IFJ), inferior parietal lobule (IPL), temporo-parietal junction (TPJ), insula, thalamus and amygdala (see Figure 1C). Areas were chosen to correspond to the modality and task of the current study (auditory and task-irrelevant, see Kim, 2014 for details). In a second step, averaged betas of the found clusters were extracted for deviant, standard and control stimulus and z-standardized in order to account for differences in raw beta values between regions. For clusters comprising several distinct regions, we extracted the cluster averages using significant voxels encompassed in the original mask templates. Then, adaptation-related activity was computed as control – standard and prediction-related activity as deviant – control (see Figure 1B). These differences were then subjected to a repeated-measures ANOVA to check whether adaptation-related and prediction-related activity varied with brain region. When applicable, violations of sphericity

were corrected using the Greenhouse-Geisser procedure and corrected *p*-values as well as $\hat{\varepsilon}$–values are reported. Two-sided *t*-tests were used to follow up significant interactions.

Results

Behavioral Data

Performance on the duration task was very high, indexed by an average hit rate of 0.92 (SD = 0.15), an average false-alarm rate of 0.003 (SD = 0.007), and an average *d'* of 4.59 (SD = 0.77), indicating that participants were able to comply with the task easily.

fMRI Data

Main effects of mismatch processing. The cluster-based permutation revealed bilateral clusters of significant mismatch processing in the auditory cortex, including STG and Heschl's gyrus (right: $p < .001$; left: $p < .001$), the ACC/SMA (right: $p = .01$; left: $p = .002$), the IFJ (right: $p = .003$; left: $p = .002$) and the AI (right: $p = .008$; left: $p = .006$). Furthermore, a significant cluster was found in the left IPL ($p = .009$). Please see Figure 2 for a visualization of clusters and beta-values and Table 1 for peak coordinates, *t*-statistics, and number of voxels (k) of the effects.

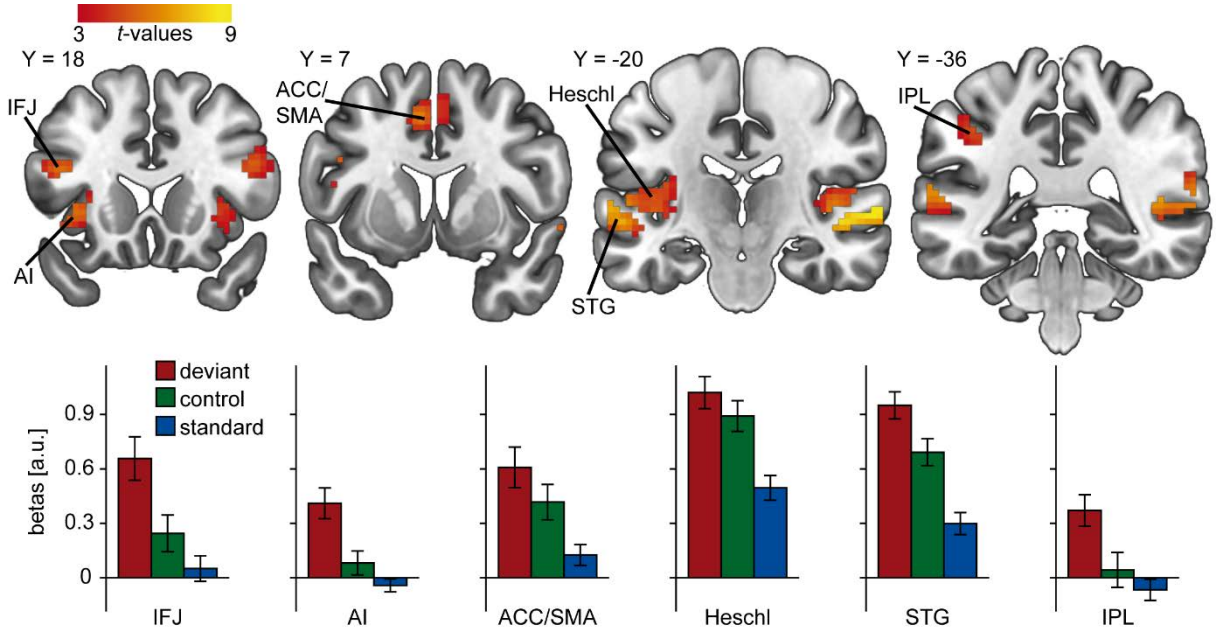

Figure 2. Auditory mismatch responses in the brain. (A) Clusters found in the cluster-based permutation comparing deviant and standard stimulus. (B) Mean beta values extracted from the clusters found. The deviant, standard and control stimulus are displayed. ACC/SMA: anterior cingulate cortex/supplementary motor area, AI: anterior insula, IFJ: inferior frontal junction, IPL: inferior parietal lobule, STG: superior temporal gyrus.

Table 1. fMRI results of the oddball contrast. ACC/SMA: anterior cingulate cortex/supplementary motor area, AI: anterior insula, IFJ: inferior frontal junction, IPL: inferior parietal lobule, STG: superior temporal gyrus.

Lobe	Area	Hemisphere	Peak MNI coordinates			*t*-statistics		k
			x	y	z	max(*t*)	mean(*t*)	
Temporal	STG	R	63	-18	0	9.51	5.63	286
		L	-54	-3	-6	7.80	5.34	264
	Heschl	R	51	-9	0	5.87	4.54	90
		L	-57	-15	6	6.03	4.68	131
Frontal	IFJ	R	45	15	21	5.38	4.25	74
		L	-42	9	24	6.94	4.58	83
	ACC/SMA	R	6	9	51	4.73	3.85	19
		L	-9	6	48	6.04	4.16	57
Parietal	IPL	L	-39	-39	39	5.10	4.08	41
Insular	AI	R	33	24	0	5.68	4.46	42
		L	-33	21	0	6.28	4.75	49

Mechanisms of mismatch processing. We found that the contribution of the different mechanisms varied depending on the brain region. The repeated-measures ANOVA indicated a significant main effect of area ($F(5,265) = 2.54$, $p = .05$, $\hat{\varepsilon} = 0.75$) and a significant interaction of area and mechanism ($F(5,265) = 3.28$, $p = .01$, $\hat{\varepsilon} = 0.79$), while the main effect of mechanism did not reach significance ($F(1,53) = 0.03$, $p = .86$). We found significant adaptation in Heschl's gyrus ($t(53) = 4.64$, $p < .001$), STG ($t(53) = 4.52$, $p < .001$) and ACC/SMA ($t(53) = 2.84$, $p = .006$), while in the AI ($t(53) = 1.81$, $p = .08$), IPL ($t(53) = 1.08$, $p = .29$) and IFJ ($t(53) = 1.57$, $p = .12$), adaptation did not reach significance, see Figure 3A. In contrast, we observed prediction in the STG ($t(53) = 3.02$, $p = .004$), AI ($t(53) = 3.75$, $p < .001$), IPL ($t(53) = 2.93$, $p = .005$) and IFJ ($t(53) = 3.18$, $p = .002$), while no significant prediction was found in Heschl's gyrus ($t(53) = 1.39$, $p = .17$) and ACC/SMA ($t(53) = 1.42$, $p = .16$).

In order to test how the relative contribution of the mechanisms differs between areas, we computed the difference between adaptation-related and prediction-related activity. Mechanisms in Heschl's gyrus differed significantly from AI ($t(53) = -3.34$, $p = .002$), IPL ($t(53) = -2.48$, $p = .02$) and IFJ ($t(53) = -2.57$, $p = .01$), STG differed significantly from AI ($t(53) = -2.60$, $p = .01$) and IFJ ($t(53) = -2.38$, $p = .02$). No other differences reached significance (all $p > .05$). See Figure 3B for a visualization of differences between cortical regions.

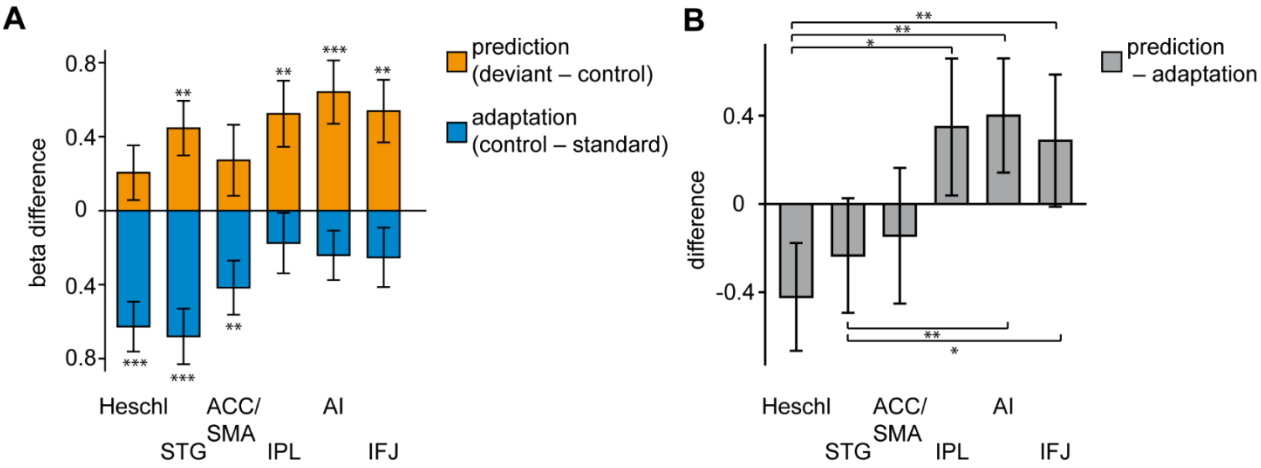

Figure 3. Mechanisms of mismatch generation. (A) Adaptation and prediction in different brain regions. Prediction-related activity is computed by substracting activity elicited by the control from the deviant. Adaptation-related activity is computed by substracting activity elicited by the standard from the control. Note that positive prediction-related activity is plotted upwards and positive adaptation-related activity is plotted downwards. (B) Relative contribution of the mechanisms, negative values correspond to a surplus of adaptation in the corresponding brain area, while positive values correspond to a surplus of prediction. Error bars depict standard error of the mean. IFJ: inferior frontal junction, AI: anterior insula, ACC/SMA: anterior cingulate cortex/supplementary motor area, STG: superior temporal gyrus, IPL: inferior parietal lobule, Asteriks correspond to the *t*-tests reported in the main text with * p < .05, ** p < .01, *** p < .001.

Discussion

In this study, we investigated the contribution of different mechanisms to explain increased deviance-related brain activation in humans. We found a hierarchical increase of the relation of predictive mechanisms vs. adaptation from primary auditory cortex across secondary auditory cortex to higher frontal and parietal regions.

Our first analytical step, in which we compared oddball and standard stimuli, confirmed deviance-related activation in most of our ROIs. This includes bilateral Heschl's gyrus and STG, which are commonly linked to auditory processing. Heschl's gyrus encompasses the primary auditory cortex (Costa et al., 2011), while the STG is involved in higher-order auditory

processing (Binder et al., 2000). The effects in both areas have been linked to the modulatory influences of the dorsal attention network (Kastner & Ungerleider, 2000), as well as preattentive change detection (Näätänen et al., 2007). Besides effects in sensory processing areas, we found several distinct clusters in frontal and parietal areas as well as the insula. In line with the meta-analytic results of Kim (2014) for task-irrelevant oddball studies, activations were mainly detected in regions belonging to the ventral attention network, which is involved in orienting attention to salient events and thus alerting the organism to environmental changes (Corbetta & Shulman, 2002; Sestieri et al., 2012). This includes the AI and ACC/SMA (Eckert et al., 2009; Yeo et al., 2011), which are also strongly involved in detecting salient events and initiating task-based attention (Goulden et al., 2014; Menon & Uddin, 2010; Shackman et al., 2011). Furthermore, we found strong bilateral IFJ activity. The IFJ is involved in the dorsal fronto-parietal network modulating goal-directed attention in sensory areas in a top-down fashion (Kim, 2014; Yeo et al., 2011), but also in a network activated by unexpected salient environmental changes (Sestieri et al., 2012). This duality fits with the suggestion that the IFJ presents a dynamic region integrating information from both dorsal and ventral networks (Asplund et al., 2010). In addition to these activations, we also found deviance-related effects in the left IPL, which is part of a fronto-parietal control network (Cole et al., 2013; Corbetta & Shulman, 2002; Yeo et al., 2011), probably involved in indexing expectancy violations (O'Connor et al., 2010).

These deviance-related effects could be explained to varying degrees by adaptation- and prediction-related activity. We found significant contributions of adaptation in Heschl's gyrus in line with previous research indicating sensory refractoriness effects in this area (Opitz et al., 2005), while prediction did not reach significance. However, this does not mean that primary auditory cortex does not show prediction-related activation (Opitz et al., 2005), but that adaptation is – averaged across the deviance-related cluster – the primary driver of information processing. In contrast to primary auditory cortex, prediction-related activity was significantly

observed in the STG in accordance with previous studies showing an increase of predictive processes along the auditory processing hierarchy (Laufer et al., 2008; Opitz et al., 2005; Parras et al., 2017).

Furthermore, in the AI, IFJ and IPL, a significant prediction effect was found, but no adaptation effect. This fits well with studies showing a dominant role of these regions during various predictive processes (Allen et al., 2016; Dürschmid et al., 2016; Geuter et al., 2017; O'Connor et al., 2010; Siman-Tov et al., 2019). Surprisingly, we found no significant prediction-related activity in ACC/SMA, probably due to the task-irrelevant oddball paradigm chosen here, which considerably differs from the paradigms linking ACC to predictive processing (Alexander & Brown, 2019). Furthermore, even though we used a large sample of participants, a further increase of sample size could probably alter results for the ACC/SMA.

Comparing the relative contribution of prediction and adaptation, we observed differences between areas mainly concerned with auditory processing and higher-order areas like the AI and IFJ. Thus, while prediction starts in auditory areas like the STG, its contribution to deviance-related effects increases on higher levels. These results are in line with the results of Dürschmid and colleagues (2016), who found an increase of predictive processing from temporal to frontal areas. Furthermore, this supposed hierarchical organization fits well with the results of Li and colleagues (2019). These authors reconstructed the temporal evolution of deviance-related responses by combining EEG and fMRI and found the information to flow from auditory cortex via the insula to the inferior frontal cortex. These findings are also in line with the proposal of hierarchical prediction error processing as a basic principle in the human brain (Clark, 2013).

While our study has many strengths, there are also limitations. We only investigated mechanisms of deviance processing during a condition where oddball stimuli had to be attended to but were not targets. Mechanisms predominantly observed during deviance processing might be modulated by task settings, thus experimentally combining task manipulations with fMRI

might help better understand which brain regions vary in their predominant mechanisms and which do not. Furthermore, we only investigated the auditory modality. Future studies should also include other sensory stimulations. Finally, future research would profit from other experimental and analytical approaches for the investigation of different mechanisms of deviance processing.

Conclusion

We observed deviance-related effects in a widespread network of different brain regions. The processes predominantly responsible for these effects varied depending on the hierarchical level of the brain region. We detected an increase in prediction-related activity and a concurrent decrease of adaptation-related activity from lower to higher hierarchical areas. These results highlight hierarchical predictive processing in the human brain.

Acknowledgments

The authors declare no competing financial interests.

References

Alexander, W. H., & Brown, J. W. (2019). The Role of the Anterior Cingulate Cortex in Prediction Error and Signaling Surprise. *Topics in Cognitive Science*, *11*(1), 119–135. https://doi.org/10.1111/tops.12307

Allen, M., Fardo, F., Dietz, M. J., Hillebrandt, H., Friston, K. J., Rees, G., & Roepstorff, A. (2016). Anterior insula coordinates hierarchical processing of tactile mismatch responses. *NeuroImage*, *127*, 34–43. https://doi.org/10.1016/j.neuroimage.2015.11.030

Ashburner, J. (2007). A fast diffeomorphic image registration algorithm. *NeuroImage*, *38*(1), 95–113. https://doi.org/10.1016/j.neuroimage.2007.07.007

Asplund, C. L., Todd, J. J., Snyder, A. P., & Marois, R. (2010). A central role for the lateral prefrontal cortex in goal-directed and stimulus-driven attention. *Nature Neuroscience*, *13*(4), 507–512. https://doi.org/10.1038/nn.2509

Binder, J. R., Frost, J. A., Hammeke, T. A., Bellgowan, P. S. F., Springer, J. A., Kaufman, J. N., & Possing, E. T. (2000). Human Temporal Lobe Activation by Speech and Nonspeech Sounds. *Cerebral Cortex*, *10*(5), 512–528. https://doi.org/10.1093/cercor/10.5.512

Clark, A. (2013). Whatever next? Predictive brains, situated agents, and the future of cognitive science. *Behavioral and Brain Sciences*, *36*(03), 181–204. https://doi.org/10.1017/S0140525X12000477

Cole, M. W., Reynolds, J. R., Power, J. D., Repovs, G., Anticevic, A., & Braver, T. S. (2013). Multi-task connectivity reveals flexible hubs for adaptive task control. *Nature Neuroscience*, *16*(9), 1348–1355. https://doi.org/10.1038/nn.3470

317 Corbetta, M., & Shulman, G. L. (2002). Control of goal-directed and stimulus-driven
318 attention in the brain. *Nature Reviews Neuroscience*, *3*(3), 201–215.
319 https://doi.org/10.1038/nrn755
320 Corbin, N., Todd, N., Friston, K. J., & Callaghan, M. F. (2018). Accurate modeling of
321 temporal correlations in rapidly sampled fMRI time series. *Human Brain Mapping*,
322 *39*(10), 3884–3897. https://doi.org/10.1002/hbm.24218
323 Costa, S. D., Zwaag, W. van der, Marques, J. P., Frackowiak, R. S. J., Clarke, S., & Saenz, M.
324 (2011). Human Primary Auditory Cortex Follows the Shape of Heschl's Gyrus.
325 *Journal of Neuroscience*, *31*(40), 14067–14075.
326 https://doi.org/10.1523/JNEUROSCI.2000-11.2011
327 Desikan, R. S., Ségonne, F., Fischl, B., Quinn, B. T., Dickerson, B. C., Blacker, D., Buckner,
328 R. L., Dale, A. M., Maguire, R. P., Hyman, B. T., Albert, M. S., & Killiany, R. J.
329 (2006). An automated labeling system for subdividing the human cerebral cortex on
330 MRI scans into gyral based regions of interest. *NeuroImage*, *31*(3), 968–980.
331 https://doi.org/10.1016/j.neuroimage.2006.01.021
332 Dürschmid, S., Edwards, E., Reichert, C., Dewar, C., Hinrichs, H., Heinze, H.-J., Kirsch, H.
333 E., Dalal, S. S., Deouell, L. Y., & Knight, R. T. (2016). Hierarchy of prediction errors
334 for auditory events in human temporal and frontal cortex. *Proceedings of the National*
335 *Academy of Sciences*, *113*(24), 6755–6760. https://doi.org/10.1073/pnas.1525030113
336 Eckert, M. A., Menon, V., Walczak, A., Ahlstrom, J., Denslow, S., Horwitz, A., & Dubno, J.
337 R. (2009). At the heart of the ventral attention system: The right anterior insula.
338 *Human Brain Mapping*, *30*(8), 2530–2541. https://doi.org/10.1002/hbm.20688
339 Garrido, M. I., Kilner, J. M., Stephan, K. E., & Friston, K. J. (2009). The mismatch
340 negativity: A review of underlying mechanisms. *Clinical Neurophysiology*, *120*(3),
341 453–463. https://doi.org/10.1016/j.clinph.2008.11.029

342 Geuter, S., Boll, S., Eippert, F., & Büchel, C. (2017). Functional dissociation of stimulus
343 intensity encoding and predictive coding of pain in the insula. *ELife*, *6*, e24770.
344 https://doi.org/10.7554/eLife.24770
345 Goulden, N., Khusnulina, A., Davis, N. J., Bracewell, R. M., Bokde, A. L., McNulty, J. P., &
346 Mullins, P. G. (2014). The salience network is responsible for switching between the
347 default mode network and the central executive network: Replication from DCM.
348 *NeuroImage*, *99*, 180–190. https://doi.org/10.1016/j.neuroimage.2014.05.052
349 Greve, D. N. (2009). *Optseq2* (Version 2.15) [Computer software].
350 https://surfer.nmr.mgh.harvard.edu/optseq/
351 Ishishita, Y., Kunii, N., Shimada, S., Ibayashi, K., Tada, M., Kirihara, K., Kawai, K., Uka, T.,
352 Kasai, K., & Saito, N. (2019). Deviance detection is the dominant component of
353 auditory contextual processing in the lateral superior temporal gyrus: A human ECoG
354 study. *Human Brain Mapping*, *40*(4), 1184–1194. https://doi.org/10.1002/hbm.24438
355 Jääskeläinen, I. P., Ahveninen, J., Bonmassar, G., Dale, A. M., Ilmoniemi, R. J., Levänen, S.,
356 Lin, F.-H., May, P., Melcher, J., Stufflebeam, S., Tiitinen, H., & Belliveau, J. W.
357 (2004). Human posterior auditory cortex gates novel sounds to consciousness.
358 *Proceedings of the National Academy of Sciences*, *101*(17), 6809–6814.
359 https://doi.org/10.1073/pnas.0303760101
360 Kastner, S., & Ungerleider, L. G. (2000). *Mechanisms of visual attention in the human cortex*
361 (Vol. 23).
362 Kiehl, K. A., Stevens, M. C., Laurens, K. R., Pearlson, G., Calhoun, V. D., & Liddle, P. F.
363 (2005). An adaptive reflexive processing model of neurocognitive function:
364 Supporting evidence from a large scale (n = 100) fMRI study of an auditory oddball
365 task. *NeuroImage*, *25*(3), 899–915. https://doi.org/10.1016/j.neuroimage.2004.12.035

366 Kim, H. (2014). Involvement of the dorsal and ventral attention networks in oddball stimulus
367 processing: A meta-analysis. *Human Brain Mapping*, *35*(5), 2265–2284.
368 https://doi.org/10.1002/hbm.22326
369 Laufer, I., Negishi, M., Rajeevan, N., Lacadie, C. M., & Constable, R. T. (2008). Sensory and
370 cognitive mechanisms of change detection in the context of speech. *Brain Structure*
371 *and Function*, *212*(5), 427–442. https://doi.org/10.1007/s00429-007-0167-8
372 Li, Q., Liu, G., Yuan, G., Wang, G., Wu, Z., & Zhao, X. (2019). Single-Trial EEG-fMRI
373 Reveals the Generation Process of the Mismatch Negativity. *Frontiers in Human*
374 *Neuroscience*, *13*. https://doi.org/10.3389/fnhum.2019.00168
375 Maess, B., Jacobsen, T., Schröger, E., & Friederici, A. D. (2007). Localizing pre-attentive
376 auditory memory-based comparison: Magnetic mismatch negativity to pitch change.
377 *NeuroImage*, *37*(2), 561–571. https://doi.org/10.1016/j.neuroimage.2007.05.040
378 May, P. J. C., & Tiitinen, H. (2010). Mismatch negativity (MMN), the deviance-elicited
379 auditory deflection, explained. *Psychophysiology*, *47*(1), 66–122.
380 https://doi.org/10.1111/j.1469-8986.2009.00856.x
381 Menon, V., & Uddin, L. Q. (2010). Saliency, switching, attention and control: A network
382 model of insula function. *Brain Structure and Function*, *214*(5–6), 655–667.
383 https://doi.org/10.1007/s00429-010-0262-0
384 Näätänen, R., Kujala, T., & Winkler, I. (2011). Auditory processing that leads to conscious
385 perception: A unique window to central auditory processing opened by the mismatch
386 negativity and related responses. *Psychophysiology*, *48*(1), 4–22.
387 https://doi.org/10.1111/j.1469-8986.2010.01114.x
388 Näätänen, R., Paavilainen, P., Rinne, T., & Alho, K. (2007). The mismatch negativity (MMN)
389 in basic research of central auditory processing: A review. *Clinical Neurophysiology*,
390 *118*(12), 2544–2590. https://doi.org/10.1016/j.clinph.2007.04.026

391 Nelken, I. (2014). Stimulus-specific adaptation and deviance detection in the auditory system:
392 Experiments and models. *Biological Cybernetics*, *108*(5), 655–663.
393 https://doi.org/10.1007/s00422-014-0585-7
394 O'Connor, A. R., Han, S., & Dobbins, I. G. (2010). The Inferior Parietal Lobule and
395 Recognition Memory: Expectancy Violation or Successful Retrieval? *Journal of*
396 *Neuroscience*, *30*(8), 2924–2934. https://doi.org/10.1523/JNEUROSCI.4225-09.2010
397 Olszowy, W., Aston, J., Rua, C., & Williams, G. B. (2019). Accurate autocorrelation
398 modeling substantially improves fMRI reliability. *Nature Communications*, *10*(1),
399 1220. https://doi.org/10.1038/s41467-019-09230-w
400 Opitz, B., Schröger, E., & Cramon, D. Y. V. (2005). Sensory and cognitive mechanisms for
401 preattentive change detection in auditory cortex. *European Journal of Neuroscience*,
402 *21*(2), 531–535. https://doi.org/10.1111/j.1460-9568.2005.03839.x
403 Parras, G. G., Nieto-Diego, J., Carbajal, G. V., Valdés-Baizabal, C., Escera, C., & Malmierca,
404 M. S. (2017). Neurons along the auditory pathway exhibit a hierarchical organization
405 of prediction error. *Nature Communications*, *8*(1), 2148.
406 https://doi.org/10.1038/s41467-017-02038-6
407 Polich, J. (2007). Updating P300: An integrative theory of P3a and P3b. *Clinical*
408 *Neurophysiology*, *118*(10), 2128–2148. https://doi.org/10.1016/j.clinph.2007.04.019
409 Schröger, E., & Wolff, C. (1996). Mismatch response of the human brain to changes in sound
410 location. *NeuroReport*, *7*(18), 3005–3008.
411 Sestieri, C., Shulman, G. L., & Corbetta, M. (2012). Orienting to the Environment: Separate
412 Contributions of Dorsal and Ventral Frontoparietal Attention Networks. In G. R.
413 Mangun (Ed.), *The Neuroscience of Attention: Attentional Control and Selection* (pp.
414 100–130). Oxford University Press.
415 https://oxford.universitypressscholarship.com/view/10.1093/acprof:oso/9780195334364
416 64.001.0001/acprof-9780195334364-chapter-0005

417 Shackman, A. J., Salomons, T. V., Slagter, H. A., Fox, A. S., Winter, J. J., & Davidson, R. J.
418 (2011). The integration of negative affect, pain and cognitive control in the cingulate
419 cortex. *Nature Reviews Neuroscience*, *12*(3), 154–167.
420 https://doi.org/10.1038/nrn2994
421 Siman-Tov, T., Granot, R. Y., Shany, O., Singer, N., Hendler, T., & Gordon, C. R. (2019). Is
422 there a prediction network? Meta-analytic evidence for a cortical-subcortical network
423 likely subserving prediction. *Neuroscience & Biobehavioral Reviews*, *105*, 262–275.
424 https://doi.org/10.1016/j.neubiorev.2019.08.012
425 Stefanics, G., Kremláček, J., & Czigler, I. (2014). Visual mismatch negativity: A predictive
426 coding view. *Frontiers in Human Neuroscience*, *8*, 666.
427 https://doi.org/10.3389/fnhum.2014.00666
428 Winkler, A. M., Ridgway, G. R., Webster, M. A., Smith, S. M., & Nichols, T. E. (2014).
429 Permutation inference for the general linear model. *NeuroImage*, *92*, 381–397.
430 https://doi.org/10.1016/j.neuroimage.2014.01.060
431 Winkler, I., & Czigler, I. (2012). Evidence from auditory and visual event-related potential
432 (ERP) studies of deviance detection (MMN and vMMN) linking predictive coding
433 theories and perceptual object representations. *International Journal of*
434 *Psychophysiology*, *83*(2), 132–143. https://doi.org/10.1016/j.ijpsycho.2011.10.001
435 Yan, C.-G., Wang, X.-D., Zuo, X.-N., & Zang, Y.-F. (2016). DPABI: Data Processing &
436 Analysis for (Resting-State) Brain Imaging. *Neuroinformatics*, *14*(3), 339–351.
437 https://doi.org/10.1007/s12021-016-9299-4
438 Yeo, B. T., Krienen, F. M., Sepulcre, J., Sabuncu, M. R., Lashkari, D., Hollinshead, M.,
439 Roffman, J. L., Smoller, J. W., Zöllei, L., Polimeni, J. R., Fischl, B., Liu, H., &
440 Buckner, R. L. (2011). The organization of the human cerebral cortex estimated by
441 intrinsic functional connectivity. *Journal of Neurophysiology*, *106*(3), 1125–1165.
442 https://doi.org/10.1152/jn.00338.2011